

A Study on Reaction Rate Factors of a Single-Step Combustion Mechanism for Gasoline HCCI Combustion

Pakawat Panuwatsuk

Department of Mechanical and Civil Engineering
Florida Institute of Technology
Melbourne, FL, USA

Gerald J. Micklow

Department of Mechanical and Civil Engineering
Florida Institute of Technology
Melbourne, FL, USA

Abstract—Homogeneous Charge Compression Ignition (HCCI) engine has been invented to achieve the advantages of both diesel and gasoline engines. HCCI engine can run with a higher compression ratio like diesel engine in order to achieve high thermal efficiency. Meanwhile, like gasoline engine, the engine produces less NO_x gas and particulate matters than diesel engine. However, there are several difficulties associated with HCCI combustion, which still require further development to the engine. The most important issues are autoignition timing and narrow operational range.

In order to develop an HCCI engine, a numerical simulation can significantly save cost, time and resources over an experimental study. KIVA3V program is chosen to simulate an HCCI engine in this study. This program is compatible chemically reactive flows in complex geometries, and featured with spray dynamics which is highly suitable for internal combustion engine. The program has been developed into several versions to suit experimental conditions. It yields essential data such as temperature, pressure, heat release, species concentrations and droplets data at any particular location of the geometry.

The main goal of this study is to obtain an accurate simulation for an HCCI combustion in KIVA3V program. KIVA3V provides a single-step combustion model with sets of reaction rate factors for some fuels. The fuels data and combustion model have been proven to work well with typical spark ignition and compression ignition engine. However, HCCI combustion has autoignition activity and relatively high residual gas content. The original reaction rate factors were derived from flame propagation and not accounted for high residual gas content. Thus, the reaction rate was overpredicted causing an excessively early combustion

The two reaction rate factors, pre-exponential factor and activation energy, are modified separately obtain precise autoignition timing for the HCCI combustion for each. Then, the simulated in-cylinder temperature and pressure from both cases are found to match the

experimental data. The modified activation energy case provided slightly more rapid heat release than the modified pre-exponential factor case.

Keywords—component; HCCI combustion; single-step combustion mechanism; KIVA-3V; gasoline.

I. INTRODUCTION

Global warming is a significant problem of the world today. Besides, internal combustion engines are one of the global warming causes but still necessary in several applications. This leads to the demands for lower emission and higher efficiency of the engines. Homogeneous Charge Compression Ignition (HCCI) engine is invented especially for enhancing efficiency and reducing emission. HCCI engine provides significantly higher efficiency than gasoline engines as the compression ratio can be higher without combustion knocks. Meanwhile, it does not produce as much particulate matter and NO_x as diesel engines do. However, HCCI engine still needs to be developed for better stability and operational range.

Numerical simulation is an alternative way to study HCCI combustion with less cost and facilities needed. With performance of present computational technologies, complex simulations can be simulated in optimal time. KIVA is one of the computer programs that is known for combustion simulations due to its ability to simulate various scenarios of chemically reactive flows and liquid sprays. In KIVA, the combustion mechanism can be modified to suit the experiment. The simplest mechanism is a single-step global mechanism. This mechanism is effective for generic gasoline and diesel engines, and consume relatively small amount of time.

Chemical kinetics model combustion may need to be modified for HCCI combustion. In HCCI combustion, the burn rate depends on reaction rate because the whole mixture theoretically ignites at the same time by its pressure and temperature. Consequently, the fuel activation energy and reaction rate need to be highly precise. Moreover, this combustion featured extremely high content of residual gas which the original combustion model does not account for. In this study, a proposed single-step combustion mechanism from Westbrook [1] is implemented. With the single-step mechanism, the fuel

activation energy and pre-exponential factor are investigated and modified for an accurate simulation of the HCCI combustion.

A. Homogeneous Charge Compression Ignition (HCCI) Engine

Internal combustion engines need to be improved relentlessly to suit the increasing demand for efficiency and regulations for emission. Two most common types of internal combustion engine, Gasoline and Diesel, have their own limitations that are barely possible to avoid. Gasoline engine has a limit on compression ratio which is an important factor affecting efficiency. Compression ratio of gasoline engine cannot exceed the point that autoignition occurs. Diesel engine, on the other hand, can support relatively high compression ratio allowing higher efficiency to be achieved. However, it produces Diesel particulate matter and NO_x which are highly harmful for health and being more controlled by automotive regulations. HCCI engine combines principles from the two engines. The engine compresses the air-fuel mixture like Gasoline engine but let it ignite with by the temperature and pressure, not initiation from a spark plug. Hence, HCCI engine can support higher compression ratio than Gasoline engine leading to a higher efficiency. Besides, HCCI engine does not emit particulate matter like Diesel does. Therefore, HCCI engine can obtain the advantages of both Diesel and Gasoline engines.

1) HCCI Combustion Characteristics

In spark-ignition combustion, heat release rate is determined by the burnt mass fraction. Meanwhile, heat release rate of HCCI combustion depends mainly on chemical reaction speed because the whole mixture theoretically burns at the same time, according to Peng's study on HCCI combustion with n-Heptane [2]. The combustion can be divided into two stages. The first stage occurs from partial oxidation of fuel molecule and its subsequent isomerization actuating a cool flame or low temperature reaction. Heat release from this stage can be less than 20%. The second stage is dominated by the formation of more active branching agents causing hot ignition.

2) Efficiency of HCCI Engine at Various Compression Ratio

Increasing compression ratio directly increases thermal efficiency of gasoline engine. In Spark Ignition (SI) engine, compression ratio cannot exceed a limit that causes autoignition. Meanwhile, in Homogeneous Charged Compression Ignition (HCCI) engine, autoignition is supposed to occur. As a result, higher compression ratio can be achieved. However, when compression ratio is changed, some variables need to be changed to maintain correct ignition timing for HCCI combustion. And, at too high compression ratio, although the thermal efficiency increases, fuel conversion efficiency may not increase due to higher heat loss and decrement in the ratio of specific heat.

An experiment from Yang [3] showed the relations between some variables, primary reference (PRF)

number, compression ratio and intake temperature, when maintaining constant ignition timing (CA50 at 5 deg TDC). If the PRF number increases, the intake temperature needed to increase to maintain the ignition timing. Increasing compression ratio could be applied with higher PRF number fuel to maintain the ignition timing.

An experiment showing the relations between PRF number, compression ratio and efficiency, when maintaining constant ignition timing (CA50 at 5 deg TDC) was performed. At a higher compression ratio, the thermal efficiency of an HCCI engine was higher. At one compression ratio, when fuel PRF number increases, the efficiency decreased due to necessarily increased intake temperature. At high compression ratio, its effect on increasing fuel conversion efficiency was be smaller due to higher heat loss, and a slight decrement of ratio of specific heat.

3) HCCI Operational Range

HCCI operational range is limited by EGR (exhaust gas recirculation) rate and fuel concentration from an n-heptane HCCI experiment [2]. In an experiment, engine load was represented by Indicated Mean Effective Pressure (IMEP). High load was determined by knocking combustion. Knocking combustion was a result of too rich mixture (low lambda) leading to rapid heat release rate which caused noise and damage. The lower load region was specified by misfire due to high concentration of H₂O and CO₂. At this condition the engine ran with intermittent misfire cycles. Although the engine could come back to normal operation occasionally, the stability of engine appears to be poor because of high number of Coefficient of Variation of IMEP (COVIMEP). Without misfire the low IMEP limit would be limited by minimum load that the engine needs to overcome which was frictional loss.

a) Effect of Intake Temperature on Operational Range

To investigate the effect of intake temperature, experiments were performed with 3 different temperatures, 105°C, 70°C, and 30°C, with other factors controlled. It was found that when intake temperature rises from 30°C to 105°C, the low load limit and high load limit were hardly affected. However, increasing intake temperature could extend the misfire limit significantly. By doing so, EGR rate could be increased further without causing misfires.

b) Effect of Compression Ratio on Operational Range

To observe the effect of compression ratio, a variable compression ratio engine is implemented to compare the operational range. Three compression ratios were investigated, 12:1, 15:1 and 18:1. It was found that increasing compression ratio greatly improved low load limit. This means higher compression ratio allowed engine to run with a leaner mixture and higher EGR rate without misfire. Nevertheless, rising compression ratio slightly worsened high load limit, which means knocking combustion occurred easier.

4) NO_x Emission Characteristics of HCCI engine

NO_x emission has been a problematic factor for a Diesel engine for a long time. As diesel engine is highly popular in mass transportation, the restriction on NO_x emission becomes more serious. To reduce NO_x from diesel engine, performance, cost and fuel economy need to be affected. HCCI engine is an alternative way to achieved high efficiency similar to diesel engine, but HCCI combustion associates with lean mixture and relatively low temperature. This means NO_x has tendency to be lower. Thus, NO_x emission investigation for HCCI engine plays an important role. A study conducted by Hailin [4] has examined NO_x emission characteristics of a CFR HCCI engine using n-Heptane as fuel.

a) Effect of Air-Fuel Ratio on NO_x Emission of HCCI Engine

There is an effective range of air-fuel ratio for an HCCI engine discussed by a study on HCCI emission characteristics [4]. From an experiment, NO_x emission could be very low at A/F from around 40 to 55. However, if A/F ratio rose over 50, the combustion efficiency would drop drastically because of a retarded ignition due to lean mixture, causing incomplete combustion. At too rich mixture, although combustion efficiency was high, NO_x increased because of high temperature.

b) Effect of Compression Ratio on NO_x Emission of HCCI Engine

In an experiment, NO_x production rose slightly and quite linearly when the compression ratio increased after 11. This showed that there was a weak effect of compression ratio on NO_x emission when the mixture was lean. However, when the compression ratio decreased from 11, NO_x emission rose rapidly before dropped again at the compression ratio of 9, when the combustion efficiency was extremely low. The rising of NO_x production at low compression ratio might be due to incomplete combustion. And the dropped of NO_x production at low combustion efficiency zone might be due to the dropped temperature.

c) Effect of EGR on NO_x Emission of HCCI Engine

There as an experiment showed that increasing EGR rate could reduce NO_x emission up to one point. In this case after 50% EGR, NO_x increased sharply, which correlated with the dropping combustion efficiency. This meant if EGR exceeded this point, the exhaust concentration would be too high causing incomplete combustion.

5) Negative Valve Overlap (NVO)

In order to obtain autoignition in HCCI engine, temperature of the mixture needs to be controlled. Exhaust gas trapping is an effective way to control the temperature of the mixture, which can be obtained by adjusting valve timing. In SI engines, positive valve overlap is widely implemented to adjust the combustion temperature and reduce NO_x emission. This overlap allows some exhaust gas from exhaust manifold to flow into the cylinder during intake period. However, in HCCI engine a large amount of exhaust

gas needs to be trapped, which exceeds ability of positive valve overlap. Thus, negative valve overlap is implemented to trap more exhaust gas. In negative valve overlap, the exhaust valve will close before the piston reaches TDC trapping some exhaust gas in the cylinder when all the valves are closed. And the intake valve will open after TDC letting intake gas flow in to blend with the trapped exhaust. Bhawe & Kraft [5] compared the effects to in-cylinder temperature of positive valve overlap and negative valve overlap. With negative valve overlap, the energy from re-compressed residual gas advanced autoignition timing and increased the temperature peak significantly.

6) Spark-Assist HCCI

In HCCI engine ignition timing control is one of the important difficulties. Spark ignition is a way to control the ignition timing effectively. However, spark plug is not used to initiate a propagating flame front like in SI engine. According to a study of spark effects on HCCI engine [6], spark is used to add some amount of energy to trigger HCCI combustion. In order to implement spark for HCCI, the pressure and temperature must be prepared in the ready state called sub HCCI critical status (sub-HCCI-CS) or HCCI-CS. From these two states, the whole mixture is ready for auto-ignition as soon as the spark triggers.

a) Spark-Assist at sub-HCCI-CS

An experiment from Wang [6] showed effect of spark on sub-HCCI-CS mixture. In the experiment, the intake was heated to 180°C for sub-HCCI-CS. In the cycle with spark, HCCI combustion was triggered due to the high rising pressure. Meanwhile, from the cycles without spark, the pressure did not rise sufficiently, which was considered misfire.

b) Spark-Assist at HCCI-CS

Another experiment from Wang [6] was performed on HCCI-CS mixture. Without spark, combustion existed but appeared to be extremely unstable. Misfires and knocks alternately occur. The engine speed changed back and forth, so did the torque output. Meanwhile, with spark, misfires disappeared, and COV reduces significantly. This meant spark succeeded to stabilize the combustion from HCCI-CS. The result could also be implied that spark could be used to smoothen the transition between SI and HCCI mode for an engine that supports two combustion modes.

c) Effects of spark timing

From Yang's study on a spark-assisted HCCI engine [7], the spark timing was varied when heat release rate, in-cylinder pressure and in-cylinder temperature were compared. In this experiment, the no-spark case insisted that the mixture was already was HCCI-CS state before the spark is applied. And the combustion from the spark was also HCCI combustion. It could be observed that spark timing could control the ignition timing as a more advanced spark led to an earlier combustion as 10% of mass fraction burnt (MFB). Besides, spark could enhance the combustion stability due to the reduced coefficient of variation.

7) Effect from Residual Gas Content

In HCCI combustion, residual is essential in order to add more energy for achieving the autoignition. The residual gas however will also change the combustion speed. According to Rhodes and Keck's study on laminar flame speed measurement [8], N₂-CO₂ diluent reduced the laminar flame speed much more than the addition of excess air does. The diluent absorbed energy and impeded the diffusion of chemical species and heat. The experiment was conducted to compare laminar flame speed between the excess air diluent containing and N₂-CO₂ diluent containing mixture. It can be found that, at the same amount, the N₂-CO₂ diluent gave a significantly slower flame speed than the air diluent. The N₂-CO₂ represented the residual gas content in an internal combustion engine. This slower flame speed due to residual gas content needs to be considered in numerical simulation of internal combustion engines including HCCI combustion.

Another study on SI engine performance prediction conducted by Micklow, Murphy and Abdel-Salam [9] also demonstrated the effects of residual gas on laminar flame speed. The cycle analysis involves laminar flame speed calculation. The residual gas appeared to slow down the flame speed. If there is any residual gas content, the calculated laminar flame speed needs to be corrected by the following equation

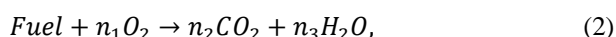
$$S_L(f) = S_L(f = 0)(1 - 2.06f^{0.77}), \quad (1)$$

where S_L is laminar flame speed and f is residual mass fraction.

B. Chemical Kinetic Modelling

A proper chemical kinetic model is highly important for an HCCI simulation. Coupled with thermodynamic model, chemical kinetic model is capable to predict the ignition timing of HCCI engine and lead to a precise ignition timing control which is a key issue of the engine. A simplified mechanism can reduce computational requirements but can overpredict the heat release rate and ignition timing. Meanwhile, a detailed mechanism can be more accurate but consume more computational resources and requires more data. To optimize the simulation, accuracy and computational resources, a study on combustion models needs to be conducted.

In some multidimensional combustion model, detail mechanisms are not suitable because of the limitation of computational performance and time. Moreover, detail mechanism may provide several details that are not necessary for the research. Thus, the global mechanism is a useful alternative way for combustion simulations. The chemical reaction for typical hydrocarbon fuels can be expressed as



where stoichiometric coefficient n_1 depends of the fuel.

The reaction rate represents one value determined from many elementary reactions occurring in the detailed mechanism. The single rate expression, obtain from Westbrook [1], is

$$k_{ov} = AT^n e^{-E_a/RT} [Fuel]^a [Oxidizer]^b. \quad (3)$$

The constants A , n , E_a , a , and b must be evaluated from experiments. The equation (3) can also be applied to non-hydrocarbon fuels. a and b are not related to stoichiometric coefficients and, in many cases, assumed to be 1. First of all, to evaluate a reaction rate, some constants are assumed, $n = 0$, $E_a = 30$ kcal/mol. The constant A must be selected so that the calculated laminar flame speed for an equivalent ratio (ϕ) matches the experimental data. For a case of n-octane, when A is chosen to be 1.15×10^{15} , the calculated laminar flame speed matches an experiment at $\phi = 1$ at atmospheric pressure. The reaction rate is expressed as

$$k_{ov} = 1.15 \times 10^{14} e^{(-30000/RT)} [C_8H_{18}]^{1.0} [O_2]^{1.0} \quad (4)$$

However, for a further ϕ , there are excessive errors in reaction rate compared to the experimental data. Another parametric study proposes a new set of constants that can reproduce the experimental flame speed at a wider range of fuel concentration. The expression for the reaction rate for n-octane is

$$k_{ov} = 4.6 \times 10^{11} e^{(-30000/RT)} [C_8H_{18}]^{0.25} [O_2]^{1.5} \quad (5)$$

The global reaction rate for iso-octane which usually represents gasoline can be expressed as

$$k_{ov} = 7.2 \times 10^{12} e^{(-40000/RT)} [C_8H_{18}]^{0.25} [O_2]^{1.5} \quad (6)$$

II. COMPUTATIONAL MODEL

A. KIVA-3V Program

KIVA-3V was used to perform the simulations in this study. KIVA is a computer program for simulating chemically reactive fluid flows and sprays using numerical calculation, which is mainly designed for internal combustion engines. KIVA was developed by Los Alamos National Laboratory operated by the University of California for the United States Department of Energy. The program was released in 1985 and has been modified into many versions. The version utilized in this study is called KIVA-3V. This program is compatible with either laminar or turbulent flows, subsonic or supersonic flows, single-phase or dispersed two-phase flows. The simulation involves mesh generation, evaporating liquid sprays, droplet collision, aerodynamic breakups, number of species and chemical reactions. It's output yields heat release, pressure, temperature, concentration of species, existing spray droplets, etc. in the mesh at each time-step. With post-processor the output can also be transformed into graphical display.

B. Simulation Setup

1) Ricardo Hydra Research Engine

The data for simulation setup is obtained from an experiment Yang [7]. A Ricardo Hydra single cylinder research engine is utilized. The engine has 450 cc swept volume, 9:1 compression ratio, bore of 80.26 mm, and stroke of 88.9 mm respectively. A direct injector from Orbital Engine Corporation Ltd. has been equipped. The intake heater is installed in the intake pipe, and set the intake temperature to 175°C. The intake is naturally aspirated. The piston consists of two parts, upper piston and lower piston, in order to equip

the optical visualizing instrument. The research studies HCCI combustion with Negative Valve Overlap (NVO) with varied ignition timing, equivalent ratio, and applying an optional spark-assist. However, only the results from only a fixed case without spark will be chosen to be simulated in KIVA-3V program.

2) Essential Data

The simulation setup is similar to a case from the mentioned experiment. The data is shown in Table I. For the simulation case, the air-to-fuel equivalent ratio (ϕ) is controlled to be 1.2. fuel is injected at 80° BTDC in NVO period, before intake period. Spark is disabled.

TABLE I. ENGINE SETUP

Valve Timing	Intake	440 CA deg ATDC	560 CA deg ATDC
	Exhaust	190 CA deg ATDC	280 CA deg ATDC
Intake heater	175 °C		
Engine speed	1600 rpm		
Oil temperature	55 °C		
Coolant temperature	100 °C		

Fig. 1 represents negative valve overlap (NVO) which is already explained in Chapter 3. During NVO, from 440° BTDC to 560° ATDC, the exhaust gas will be trapped in the cylinder and recompressed before the intake valves open and let the air flow in. This NVO is implemented in order to increase the mixture temperature with the exhaust gas. The residual gas content appears to be 55%.

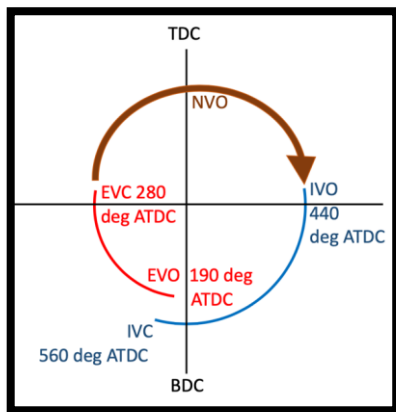


Fig. 1 Valve Timing Diagram

In the cited experiment, the injector was supplied by Orbital Engine Corporation Ltd and is a direct injection spray guided system for stratified charge SI engines. The injector sits at the middle of the cylinder head. In KIVA simulation, the droplet spray is assumed to be a hollow cone shape. Some data of the injector are obtained from a researches that uses the similar injector [10], [11]. In the experiment, there were 4 cases of injection. However, the only one most practical case for the simulation data source is chosen. The KIVA simulation of fuel spray is shown in Fig. 2.

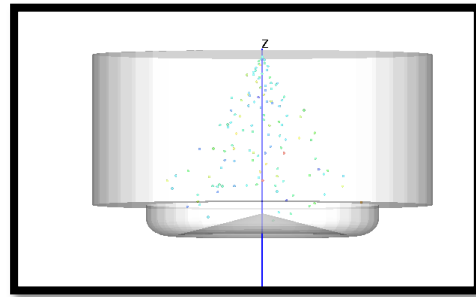


Fig. 2 Simulation of Fuel Spray

The injection, in this case, starts at 80° before TDC in NVO period. The injection takes place at recompression of exhaust stroke before intake stroke. The injection lasts until some point before the intake valves open. The duration of injection is varied to keep $\lambda = 1.2$. After the intake valves open, there is no fuel particle left. Thus, the mixture is assumed to be homogeneous.

The numerical grid for the cited engine cited is shown in Fig. 3. This grid is created based on the piston and cylinder of Ricardo Hydra engine which is implemented in KIVA-3V simulation. The numbers of blocks for the cylinder in radial, azimuthal and axial direction are 43, 44 and 80 respectively. The numbers of blocks for the piston bowl in radial, azimuthal and axial direction are 27, 44 and 10 respectively. The total number of blocks is 179255.

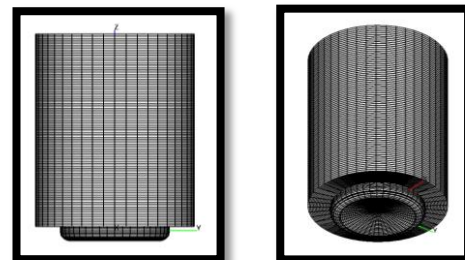
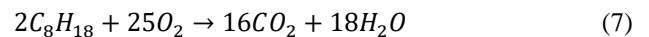


Fig. 3 Numerical grid for Ricardo Hydra engine

The single-step global mechanism from Westbrook [1] which has already been featured in KIVA-3V program is implemented. The fuel implemented is iso-octane (C8H18) whose reaction rate factors are obtained from Westbrook study [1].



The reaction rate factor for equation (7) can be calculated with equation (8).

$$k = AT^n e^{-E_a/RT} [Fuel]^a [O_2]^b \quad (8)$$

The reaction rate constants from the original study and the new cases that are going to be tested are shown in Table II, where $a = 0.25$, $b = 1.5$ and $n = 0$. Three E_a will be test in order to obtain the optimal E_a for the accurate autoignition timing. The similar process is going to perform with factor A to find another optimal reaction rate from modified A.

TABLE II. REACTION RATE FACTORS FOR GLOBAL MECHANISM OF GASOLINE AND ISO-OCTANE

Case	A	E _a (kcal/mol)	E _a /R (K)
1 (Original)	7.20E+12	40	2.0129E+04
2		42	2.1135E+04
3		44	2.2142E+04
4 (New)		To be determined	To be determined
5	7.20E+12	40	2.0129E+04
6	3.60E+12		
7	1.80E+12		
8 (New)	To be determined		

Beside the fuel oxidation, equation (9), (10) and (11) representing the formation of nitric oxide are also included.



III. RESULTS

A. Westbrook Iso-octane model [1]

Fig. 4 shows that the iso-octane model has some error in temperature when being used to simulate the HCCI combustion. First of all, the combustion started too early. And the temperature rise was too rapid. The temperature started to rise sharply around 15° before TDC which is about 10° too early compared to the experimental data. The peak temperature from the simulation was fairly close to the experiment, but it took place at about 13° too early. The overall temperature was slightly lower than in the experiment

Fig. 5 shows that overall pressure of the iso-octane model is higher than in the experiment. The pressure had a sharp rise around 10° BTDC, which made the curve split from experimental curve. The peak pressure was 7 bar too high and occurred at 9° too early. The pressure rise combined with temperature rise from Fig. 4 indicated the fact that autoignition timing was predicted to be too advanced. The relatively retarded combustion of experimental results may be caused by high residual gas content of the HCCI combustion. The current iso-octane model does not account for this extremely high residual gas content, which overpredicts the reaction rate.

B. Varied Activation Energy (E_a)

To solve the overprediction of reaction rate, one of the reaction rate factors, E_a, was varied to match the data. E_a for the original iso-octane model is 40 kcal/mol. Other two values of 42 and 44 kcal/mol were study to find an accurate matching point.

Fig. 6 indicates that increasing the activation energy (E_a) can help retard the autoignition making the temperature profile more realistic. The E_a of 42 kcal/mol gave a fairly close temperature rise to the experimental data, but the autoignition was still too

early. However, the peak temperature was slightly too low. The E_a of 44 kcal/mol, on the other hand, retarded the temperature rise excessively causing a misfire.

Fig. 7 demonstrates that increasing E_a can solve too high peak pressure problem. The E_a of 42 kcal/mol yielded lower and more retarded pressure peak than E_a of 40 kcal/mol. However, the pressure peak was still too early and the pressure rise was slightly too sharp compared to the experiment. Besides, the pressure from E_a of 44 kcal/mol did not rise enough due to the misfire. From varying E_a, the results suggested that a proper E_a for an accurate result must stay between 42 to 44 kcal/mol. To determine the proper E_a, the autoignition timings from the tested cases were compared in the next section.

1) Determination of new E_a

The new E_a was determined in order to match the autoignition timing of the experimental data. Since there was no spark involved, the start of combustion of the HCCI combustion could be determined by crank angle degree where 10% of mass fraction is burnt or CA of 10% MFB. The CA of 10% MFB of the varied E_a cases are shown in Fig. 8.

To find an optimal E_a for the accurate autoignition timing, the relation between CA of 10% MFB and E_a was curve fitted with a second order polynomial. In the curve fit equation, y represents CA of 10% MFB and x represents E_a. CA of 10% MFB of experimental data is -3°. The curve fit equation then yielded E_a of 42.67 kcal/mol which would be implemented in the following section.

2) New Activation Energy (E_a)

Fig. 9, shows that from the new temperature profile, the temperature rise became closer to the experimental data. Overall shape of temperature curve became more similar to the experimental data. The peak temperature, however, slightly dropped. The rise of temperature became more retarded and less steep than the original model, which resemble the experimental data more. However, there was some acceptable discrepancy between the experimental temperature and simulated temperature which could be caused by the limitation of data for simulation setup. And, the temperature measurement, in practical experiment, might not represent the genuine average temperature like in the simulation.

From Fig. 10, the new pressure profile became a closer shape to the experimental pressure. The excessively high pressure peak from the original model had disappeared. The overall pressure was slightly higher than the experimental data but still in an acceptable range. The new peak pressure located at the same crank angle with the experimental data.

C. Varied Pre-Exponential Factor (A)

Beside the activation energy, the pre-exponential factor was also studied. 3 values of A shown in Table 3

were implemented. From Fig. 11, it can be observed that decreasing pre-exponential factor (A) can retard the autoignition. The A of 3.6×10^{12} gave a closer temperature rise to the experimental data than the original A of 7.2×10^{12} but still too early. The A of 1.8×10^{12} gave a further retarded temperature rise than the experimental data. And, the peak pressure also dropped more. Overall, a proper A value might be in the middle of 1.8×10^{12} and 3.6×10^{12} .

Fig. 12 reinforces that decreasing A can retard the autoignition timing. The sharp pressure rise from lower A cases gave respectively more retarded autoignition timings. However, the overall pressure of the lowest A case was fairly close to the experimental data. The pressure had been slightly too high at first. Then it switched to be too low at 2° before came to a sharp rise and caught up with the experimental data later.

1) Determination of New Pre-Exponential Factor (A)

The new A was determined in the same way with Ea. The autoignition timing determined from crank angle of 10% mass burnt rate (CA of 10% MFB) was derived to compared to the experimental data. From Fig. 13, the new A turned out not necessary to be calculated since the current lowest A value coincidentally matched the autoignition timing of the experiment. The lowest A of the current comparison of 1.8×10^{12} then became the new A value for the simulation.

2) New Pre-Exponential Factor (A)

From Fig. 14, it can be seen that new exponential factor (A) yielded a more accurate temperature profile. The temperature rise became closer to the experimental study. The shape of temperature curve resembled the experimental temperature more although the peak and overall temperature was slightly lower.

Fig. 15 reinforced an improvement of the model. The excessively high pressure peak from the original model had been eliminated. The sharp rise of pressure from new model retarded to be closer to the experiment. The new pressure profile resembled the experimental data more despite some mismatch of rising and dropping near TDC. The overall pressure was still slightly higher than the experimental data.

3) Comparison Between Original and New Models

Table III compares the original set of variables to the two new sets, one was determined from new Ea and the other is determined from new A.

TABLE III. COMPARISON BETWEEN ORIGINAL AND NEW MODELS

Case	A	E _a (kcal/mol)	E _a /R (K)
Original	7.20E+12	40	2.0129E+04
Modified E _a		42.67	2.1472E+04
Modified A	1.8E+12	40	2.0129E+04

From Fig. 16, the both models from new activation energy (Ea) and new pre-exponential factor (A) yielded more accurate temperature profiles than the original model. The temperature rise of the optimal A model was more retarded than the one from optimal Ea model. However, the optimal A model gave a better slope of temperature rise. The optimal Ea model yielded a too steep temperature rise but at the more precise timing than the optimal A model.

Fig. 17 reinforced the more accurate pressure profile from both 2 new models compared to the original model. Pressure profile of both models resembled the experimental study despite some mismatch before TDC. The pressure profile also agreed with temperature profile that optimal A model gave a less steep heat release than optimal Ea model. There was some acceptable discrepancy between simulated pressures and experimental pressure. This may be due to the single-step mechanism which can represent the combustion to a certain accuracy. In the practical HCCI combustion, there are many intermediate species which play important role in heat release according to a detailed mechanism study [12]. In different stages of combustion, the species affect heat release in different ways. A detailed mechanism may be able to reduce the discrepancy.

4) Temperature Sensitivity of the New Models

From the reaction rate equation (8), with temperature order of 0 and the species term grouped, the reaction rate can be expressed as equation (12). The term that contains variable A and Ea is then investigated at a range of interested temperature to explain the difference of temperature rise between 2 new models.

$$k_{ov} = AT^n e^{-E_a/RT} [Fuel]^a [Oxidizer]^b \quad (12)$$

From Fig. 18, it can be seen that reaction rate of modified Ea case appears to be higher than modified A case for the whole range of temperature. This supports Fig. 16 from last section that modified Ea case had a steeper temperature rise than the modified A case from 0° to 10° crank angle.

IV. CONCLUSION

The goal for this study is to study effects of reaction rate factors to improve the accuracy of HCCI combustion simulation on KIVA3V. Amsden [13] proposed a single-step global mechanism as a model for combustion in KIVA3. The fuel library from KIVA3 was obtained from Westbrook's study [1]. This model works well with spark ignition combustion in a certain range of equivalent ratio. However, HCCI combustion has a different characteristic due to autoignition activity and high residual gas content. The original model overpredicted the reaction rate causing excessively advanced the autoignition timing. This indicated that reaction rate calculation needed to be modified to suit the conditions of HCCI combustion.

Two cases of modified reaction rate were achieved, one case with an increased activation energy another case with a decreased pre-exponential factor. The

accurate autoignition timing was achieved. The pressure and temperature profile from both new reaction rates were investigated to be in an acceptable range.

The difference between the two cases has been observed. Reducing reaction rate by modifying pre-exponential factor (A) gave a steeper temperature and pressure rise than modifying activation energy (E_a) due to the temperature sensitivity of the reaction rate.

REFERENCES

- [1] C. K. Westbrook and F. L. Dryer, "Chemical kinetic modeling of hydrocarbon combustion," *Prog. Energy Combust. Sci.*, vol. 10, no. 1, pp. 1–57, 1984.
- [2] Z. Peng, H. Zhao, T. Ma, and N. Ladommatos, "Characteristics of homogeneous charge compression ignition (HCCI) combustion and emissions of n-heptane," *Combust. Sci. Technol.*, vol. 177, no. 11, pp. 2113–2150, 2005.
- [3] R. Yang, D. Hariharan, S. Zilg, S. Mamalis, and B. Lawler, "Efficiency and emissions characteristics of an HCCI engine fueled by primary reference fuels," *SAE Int. J. Engines*, vol. 11, no. 6, pp. 993–1006, 2018.
- [4] H. Li, W. S. Neill, H. Guo, and W. Chippior, "The NO_x and N₂O emission characteristics of an HCCI engine operated with n-heptane," *J. energy Resour. Technol.*, vol. 134, no. 1, 2012.
- [5] A. Bhawe, M. Kraft, F. Mauss, A. Oakley, and H. Zhao, "Evaluating the EGR-AFR operating range of a HCCI engine," SAE Technical paper, 2005.
- [6] Z. Wang, J.-X. Wang, S.-J. Shuai, G.-H. Tian, X. An, and Q.-J. Ma, "Study of the effect of spark ignition on gasoline HCCI combustion," *Proc. Inst. Mech. Eng. Part D J. Automob. Eng.*, vol. 220, no. 6, pp. 817–825, 2006.
- [7] C. Yang, "Investigation of combustion and performance characteristics of CAI combustion engine with positive and negative valve overlap." Brunel University School of Engineering and Design PhD Theses, 2008.
- [8] D. B. Rhodes, "Laminar burning speed measurements of indolene-air-diluent mixtures at high pressures and temperatures." Massachusetts Institute of Technology, Department of Mechanical Engineering, 1981.
- [9] G. J. Micklow, B. Murphy, and T. Abdel-Salam, "An Efficient Thermodynamic Cycle Analysis for the Performance Prediction of Fuel Induced Spark Ignition Engines," SAE Technical Paper, 2008.
- [10] S.-H. Jin, M. J. Brear, G. Zakis, H. C. Watson, and C. Zavier, "Transient behaviour of the fuel spray from an air-assisted, direct fuel injector,"

in *Aust Fluid Mech Conf*, 2004.

- [11] S. Leighton and S. Ahern, "Fuel Economy Advantages on Indian 2-stroke and 4-stroke Motorcycles Fitted with Direct Fuel Injection," SAE Technical Paper, 2003.
- [12] M. Jia and M. Xie, "A chemical kinetics model of iso-octane oxidation for HCCI engines," *Fuel*, vol. 85, no. 17–18, pp. 2593–2604, 2006.
- [13] A. A. Amsden, "KIVA-3: A KIVA program with block-structured mesh for complex geometries," Los Alamos National Lab., NM (United States), 1993.

V. APPENDIX

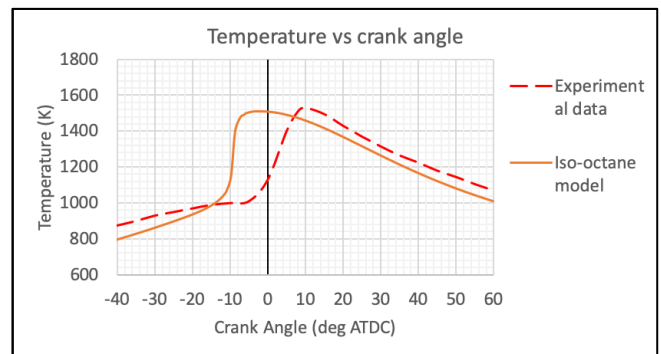


Fig. 4 Temperature Profile from Iso-Octane Model

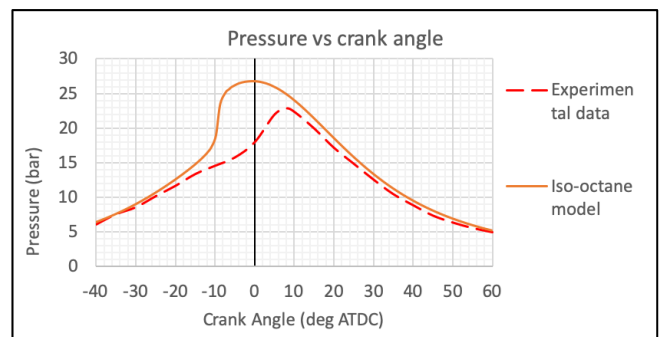


Fig. 5 Pressure Profile from Iso-Octane Model

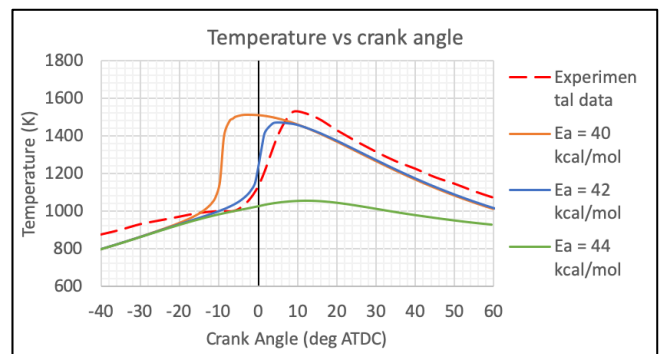


Fig. 6 Temperature Profile from Simulations with Varied E_a

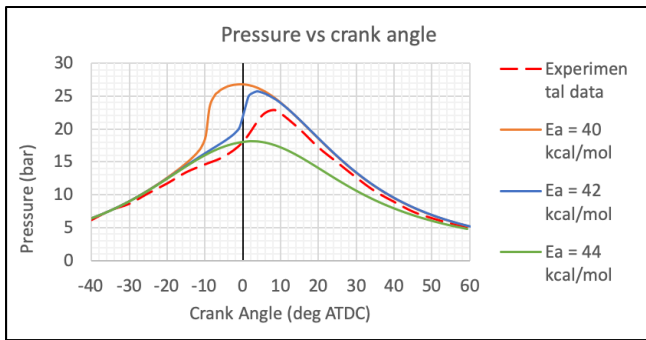


Fig. 7 Pressure Profile from Simulations with Varied Ea

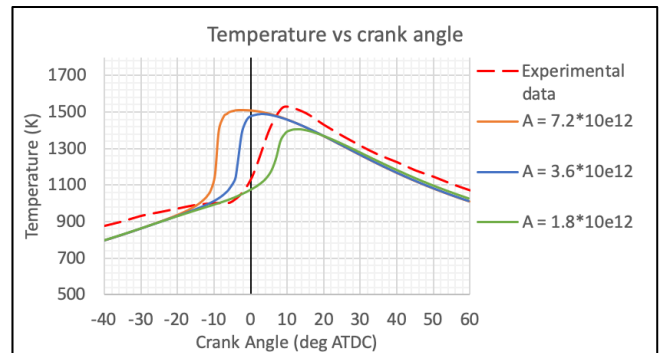


Fig. 11 Temperature Profile from Varied A

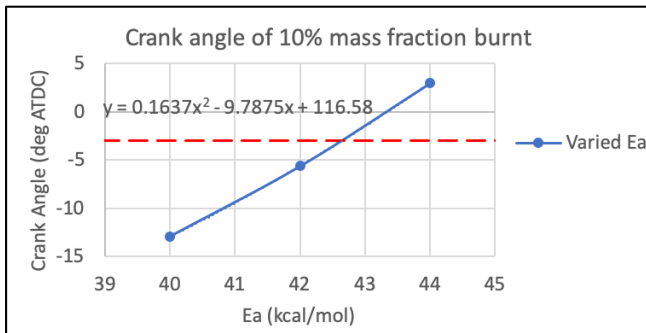


Fig. 8 Autoignition Timing Comparison for Varied Ea

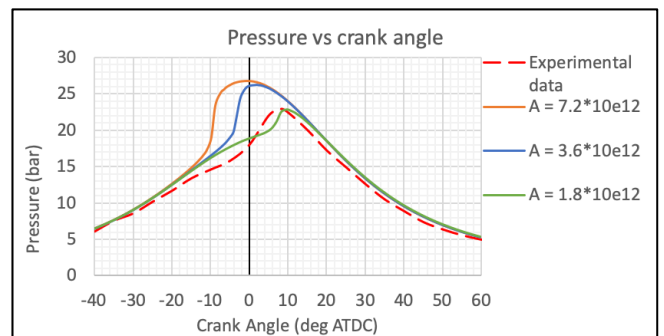


Fig. 12 Pressure Profile from Varied A

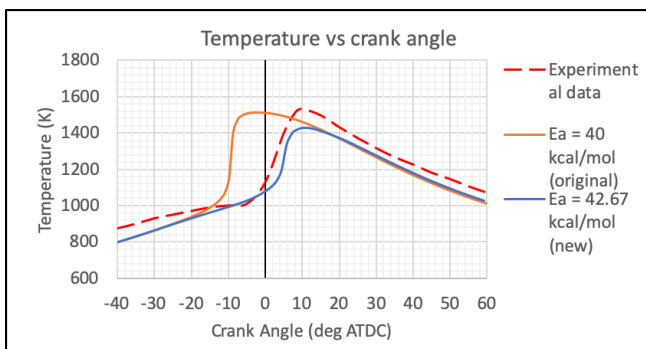


Fig. 9 Temperature Profile from New Activation Energy

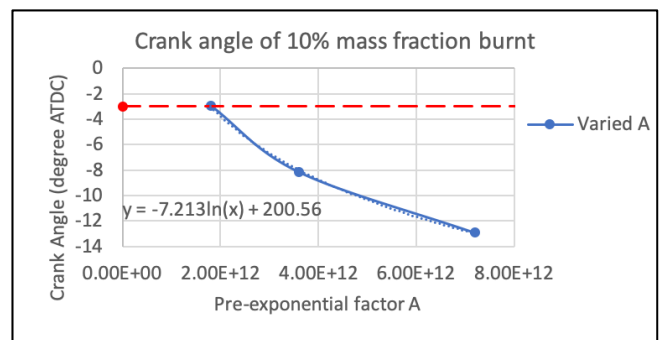


Fig. 13 Autoignition Timing Comparison for Varied A

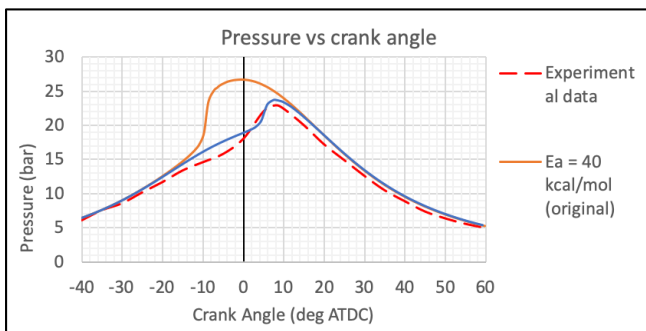


Fig. 10 Pressure Profile from New Activation Energy

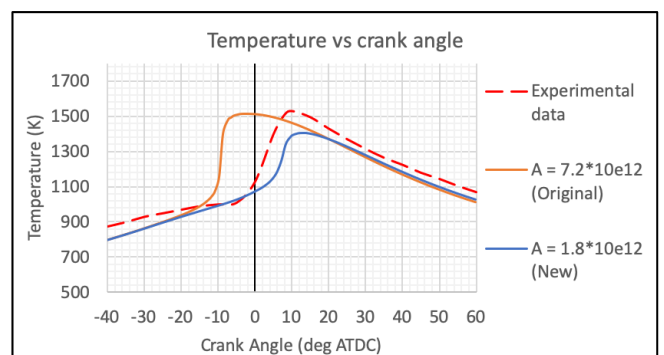


Fig. 14 Temperature Profile from New A

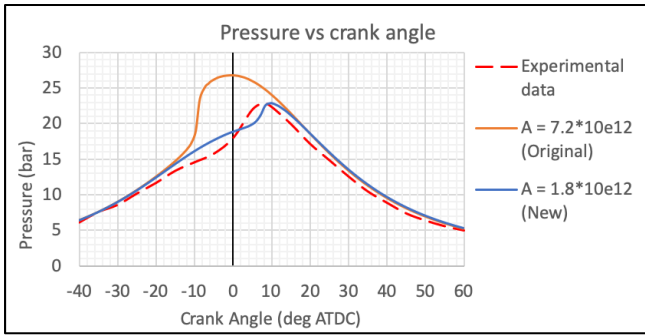


Fig. 15 Pressure Profile from New A

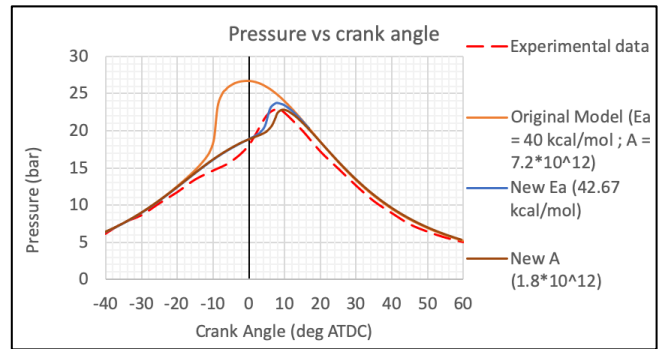


Fig. 17 Pressure Profile from Original and New Models

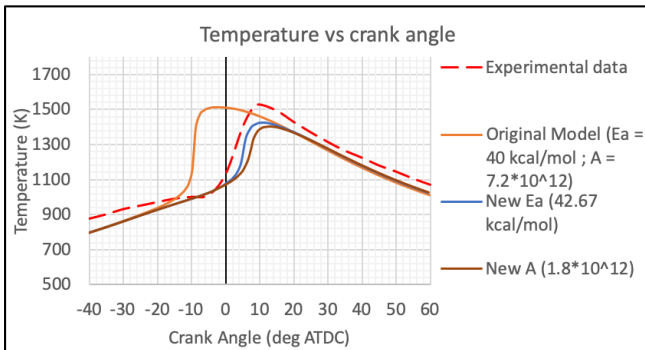


Fig. 16 Temperature Profile from Original and New Models

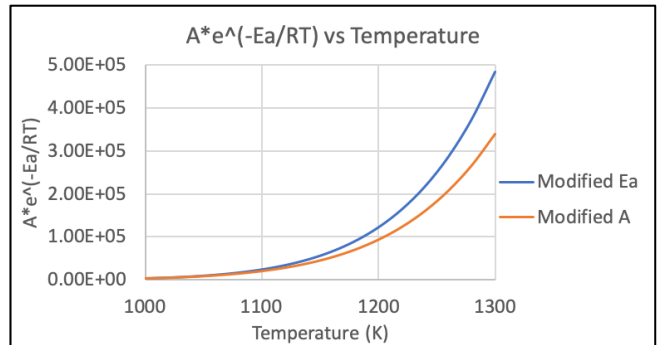


Fig. 18 Effects of Temperature on Reaction Rate Term of Modified Ea and Modified A Case